

# Hydrogen and magnesium incorporation on *c*-plane and *m*-plane GaN surfaces

John E. Northrup

Palo Alto Research Center, 3333 Coyote Hill Road, Palo Alto, California 94304, USA

(Received 16 September 2007; published 14 January 2008)

The effect of hydrogen on Mg incorporation for both polar and nonpolar GaN surfaces is explored using density functional total energy calculations. A thermodynamic approach is employed, with chemical potentials appropriate for realistic growth conditions. It is shown that hydrogen stabilizes new Mg-rich surface reconstructions for both the (0001) and (10 $\bar{1}$ 0) surfaces. Hydrogen greatly enhances the stability of Mg-rich reconstructions of the *m* plane. Experimental results for *p*-type doping obtained in growth on both the *m*-plane and *c*-plane surfaces can be understood on the basis of these results. A laterally contracted row model for the GaN(10 $\bar{1}$ 0) surface is shown to be energetically favorable in Ga-rich conditions.

DOI: 10.1103/PhysRevB.77.045313

PACS number(s): 68.35.B-

## I. INTRODUCTION

There continues to be a very high degree of interest in the group-III nitride materials and alloys. The interest is driven in part by the prospects of solid state lighting employing light emitting diodes built in this material system. Efforts are also underway to extend the range of lasing wavelengths that can be utilized. One key to continued progress is obtaining greater understanding and more control over growth. This is seen to be of particular importance when one considers that dopants such as Mg can give rise to significant alterations of the growth morphology and the growth rate.<sup>1,2</sup> It is therefore important to understand how Mg affects the GaN surface during growth. It is also known that Mg doping of GaN depends on the orientation of the growth surface.<sup>3</sup> This supplies another reason to analyze Mg doping from a surface science perspective, and that is an objective of this work. We have performed first-principles calculations for GaN surfaces on which both Mg and H are present. We attempt to understand Mg incorporation on both the *m*-plane and *c*-plane surfaces for growth conditions in which hydrogen may be present or absent.

Growth of the group-III nitrides is currently being pursued on a variety of surface orientations including the *c*-plane (0001) and *m*-plane (10 $\bar{1}$ 0). Blue-emitting lasers have been fabricated on both types of surfaces.<sup>4-6</sup> The *m* plane is a nonpolar growth surface and is attractive because of the absence of polarization fields in devices grown on such a surface. Growth of GaN can proceed under various conditions. In metal-organic chemical vapor deposition (MOCVD), the growth temperature is typically  $\sim 1300$  K and the total pressure, arising from copious quantities of NH<sub>3</sub> in the reactor, can be 1 atm or even higher.<sup>4</sup> Another set of growth conditions arises in molecular beam epitaxy (MBE), which takes place at a growth temperature of  $\sim 900$  K and with a low pressure in the growth chamber.

In material grown by MOCVD, hydrogen enters the bulk material and forms a complex with the Mg acceptor.<sup>7-9</sup> Activation of the material is therefore required to obtain *p*-type doping. In contrast, for laser-quality material grown by MBE, no such activation is required to achieve high levels of *p*-type doping.<sup>10</sup> Nevertheless, hydrogen has been observed to affect Mg incorporation on the *c* plane for MBE growth at

temperatures of  $\sim 900$  K.<sup>3</sup> Based on the present calculations, we provide an explanation on how hydrogen can reduce the required Mg flux needed to obtain Mg incorporation.

In material grown by MOCVD, extended defects such as inversion domains form if the Mg concentration in the material is too high.<sup>1,11</sup> These defects limit the doping level that can be achieved. Although the origin of the inversion is not completely understood, it seems clear that in some cases, the nucleation occurs at the surface. It is therefore important to understand the behavior of Mg on GaN surfaces in MOCVD conditions, and that requires considering conditions in which hydrogen and magnesium are present together on the surface.

## II. METHODS

Calculations were performed using the local density approximation in conjunction with first-principles pseudopotentials.<sup>12-15</sup> A plane-wave basis is employed, with an energy cutoff for the basis states equal to 60 Ry. The 3*d* electrons of gallium are included as valence electrons. The dissociation energy of a GaNH<sub>6</sub> molecule into GaH<sub>3</sub> and NH<sub>3</sub> molecules changes by less than 0.01 eV when increasing the cutoff energy from 60 to 80 Ry. A Monkhorst-Pack grid of **k** points is employed to sample the Brillouin zone.<sup>16</sup> Calculations for 1  $\times$  2 [*c*(2  $\times$  6)] unit cells on the *m* plane employ a 4  $\times$  4  $\times$  1 [2  $\times$  2  $\times$  1] grid of **k** points. For the 2  $\times$  2 calculations of the *c* plane, a 4  $\times$  4  $\times$  1 sampling grid is employed.

The relative stability for structures having differing stoichiometry is determined by the calculation of chemical potential dependent formation energies.<sup>17,18</sup> In this approach, chemical potentials are introduced for Mg, H, Ga, and N. The nitrogen chemical potential can be eliminated in favor of the Ga chemical potential by invoking the conditions for equilibrium with bulk GaN;  $\mu_{\text{Ga}} + \mu_{\text{N}} = \mu_{\text{GaN(bulk)}}$ . The Mg chemical potential can be varied but is required to be less than or equal to the value that would enable precipitation of Mg<sub>3</sub>N<sub>2</sub>,  $\mu_{\text{Mg}} < 1/3 (\mu_{\text{Mg}_3\text{N}_2(\text{bulk})} - 2\mu_{\text{N}})$ . The energy of Mg<sub>3</sub>N<sub>2</sub> was determined in prior work.<sup>19</sup> The hydrogen chemical potential depends on the temperature and partial pressure of hydrogen in the growth chamber, and its calculation is discussed elsewhere.<sup>20</sup>

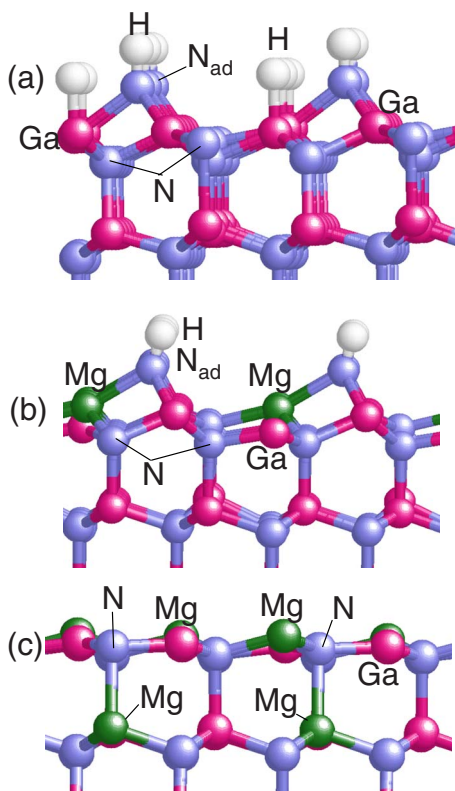


FIG. 1. (Color online) Structural models of the GaN(0001) surface. (a) The  $N_{ad}+2H$  surface comprises 0.25 ML N adatoms in H3 sites, and 0.5 ML H atoms saturating the dangling bonds on the N adatoms and the Ga rest atoms. (b) The  $N_{ad}+Mg+H$  surface has 0.25 ML Mg, each bonded to four N atoms. The dangling bond on the N adatom is saturated by hydrogen. The electron counting rule is satisfied when the Ga dangling bond on the rest atom is empty. (c) The 3Mg surface comprises 0.75 ML of Mg, with 0.5 ML of Mg in the top layer and 0.25 ML in the third layer. The dangling bonds on the Mg and Ga atoms are completely empty.

For the (0001) surfaces, a  $2 \times 2$  unit cell is employed. The slab thickness corresponds to four double-layer layers of GaN, with fractionally charged hydrogen atoms saturating the N atoms on the back side of the slab. For example, in the  $N_{ad}+2H$  structure shown in Fig. 1(a), the  $2 \times 2$  unit cell contains 16 Ga atoms, 17 N atoms, 2 H atoms, and 4 pseudohydrogen atoms. Structures with one and three Mg atoms in each  $2 \times 2$  cell are shown in Figs. 1(b) and 1(c).

For the (10 $\bar{1}$ 0) surfaces, a supercell having  $1 \times 2$  symmetry is adopted for most of the calculations. The  $1 \times 2$  cell is spanned by lattice vectors  $\mathbf{e}_1 = \mathbf{c}$  and  $\mathbf{e}_2 = 2\mathbf{a}$ , where  $\mathbf{c}$  is the usual lattice constant of GaN in the [0001] direction and the vector  $\mathbf{a}$  (of length of 3.17 Å) points along the  $\langle 11\bar{2}0 \rangle$  direction. The vectors  $\mathbf{c}$  and  $2\mathbf{a}$  are indicated in Fig. 2. For an ideal  $m$ -plane surface, a  $1 \times 2$  cell contains two Ga-N dimers. A larger cell, having a  $c(2 \times 6)$  symmetry, is employed to model a laterally contracted Ga bilayer structure appropriate for the Ga-rich  $m$  plane. In this case, the lattice vectors are  $\mathbf{e}_1 = -\mathbf{c} + 3\mathbf{a}$  and  $\mathbf{e}_2 = \mathbf{c} + 3\mathbf{a}$ . A top view of such a structure in the  $c(2 \times 6)$  cell is shown in Fig. 2. This structure will be discussed more fully in Sec. IV.

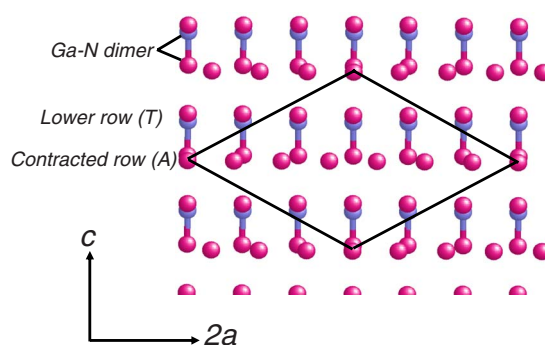


FIG. 2. (Color online) A top view of an  $m$ -plane surface is shown. The vectors  $\mathbf{c}$  and  $2\mathbf{a}$  span a  $1 \times 2$  unit cell that contains two Ga-N dimers. The  $c(2 \times 6)$  cell employed to model the laterally contracted bilayer is indicated by solid lines. A  $c(2 \times 6)$  cell contains six Ga-N dimers. The specific structure shown is a laterally contracted bilayer structure. Each  $c(2 \times 6)$  cell contains seven Ga atoms in the contracted row (row A) and six Ga atoms in the lower row (row T). Atoms in row T are bonded to N atoms.

### III. EFFECT OF HYDROGEN ON GaN(0001) SURFACES GROWN AT LOW TEMPERATURE

In studies of the MBE growth of GaN(0001), Ptak *et al.* observed that the presence of hydrogen could increase the bulk Mg concentration, determined by secondary-ion-mass spectroscopy, under some growth conditions.<sup>3</sup> For growth temperatures near 920 K, the introduction of hydrogen enabled Mg doping to occur at a lower Mg flux, but at higher Mg fluxes, the addition of hydrogen did not substantially alter the Mg concentration. The reasons for this behavior have not been understood completely. Here, we present an explanation for this finding. The argument has two components, one involving surface energetics and one related more to kinetics. The energetic component, to be discussed in detail below, is that the presence of hydrogen stabilizes Mg-containing surface reconstructions at a lower Mg flux than required in the absence of hydrogen. Put another way, when the Mg chemical potential is low, the addition of H stabilizes Mg-rich reconstructions that would otherwise be unstable. The kinetic part of the argument is that incorporation occurs because a small fraction of the Mg atoms present on the surface at a given time become kinetically trapped in the bulk as each layer is overgrown. We may write the Mg concentration in terms of the surface coverage  $\theta_{Mg}$ , the number of bulk Ga sites  $N_{bulk}$ , and the captured fraction  $f_{cap}$ ,  $[Mg] = N_{bulk} \theta_{Mg} f_{cap}$ . A typical value of the captured fraction is  $10^{-3}$ .<sup>3,21</sup> The captured fraction  $f_{cap}$  depends on temperature and growth rate. When kinetics are important, the captured fraction may become *larger* as the temperature *decreases*. This is because it is energetically more favorable for a Mg atom to reside near the surface than in the bulk. If the substrate temperature is low, then Mg atoms buried by the overgrowth cannot diffuse back to the surface and remain incorporated.

The energetic component of the argument relies on the results presented in Fig. 3. Figure 3(a) shows the relative energetics as a function of Mg chemical potential for condi-

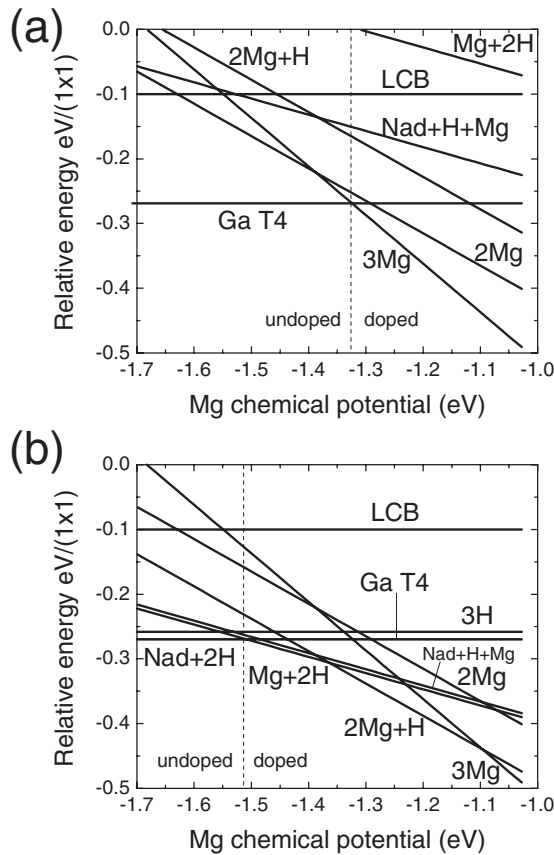


FIG. 3. The relative formation energies for Mg and H reconstructions of the GaN(0001) surface are plotted as a function of Mg chemical potential for two different hydrogen pressures. In both cases, Ga-rich growth conditions are assumed,  $\mu_{\text{Ga}} = \mu_{\text{Ga(bulk)}} - 0.2$  eV. In both cases, the temperature is 920 K. Under such conditions,  $\text{Mg}_3\text{N}_2$  will precipitate when  $\mu_{\text{Mg}}$  becomes larger than  $-1.05$  eV. In (a), the hydrogen pressure is low,  $p_{\text{H}} = 10^{-10}$  atm. This corresponds to  $\mu_{\text{H}} = -1.57$  eV at this temperature. In (b), the hydrogen pressure is much higher,  $p_{\text{H}} = 10^{-3}$  atm. This translates into  $\mu_{\text{H}} = -1.0$  eV. Note that in case (b), where H is abundant, the transition from a surface with no Mg to a surface containing Mg occurs at a lower Mg chemical potential. For the H-rich surface, a transition from the  $\text{N}_{\text{ad}}+2\text{H}$  structure to the  $\text{Mg}+2\text{H}$  structure occurs upon increasing the  $\mu_{\text{Mg}}$  above  $-1.53$  eV.

tions of low  $\mu_{\text{H}}$ . Mg chemical potentials are measured here with respect to bulk Mg. When  $\mu_{\text{Mg}}$  is low, a bare GaN surface, the  $2 \times 2$  Ga T4 adatom model for these growth conditions, is most stable.<sup>22</sup> Then, as  $\mu_{\text{Mg}}$  is increased, there is a transition to a surface having 0.75 ML of Mg atoms. This reconstruction, denoted 3Mg and shown in Fig. 1(c), was recently reported by Sun *et al.*<sup>23</sup> The transition occurs at  $\mu_{\text{Mg}} = -1.33$  eV, a value that is 0.3 eV below that needed to precipitate  $\text{Mg}_3\text{N}_2$ . Now, let us consider the effect of adding hydrogen. Figure 3(b) shows the relative surface energies calculated for a higher value of  $\mu_{\text{H}}$ . The energies shown there correspond to a chemical potential for hydrogen equal to  $-1.0$  eV. The hydrogen chemical potential is given relative to the value at  $T=0$ .<sup>20</sup> Now, when  $\mu_{\text{Mg}}$  is very low, the GaN surface adopts the  $\text{N}_{\text{ad}}+2\text{H}$  surface shown in Fig. 1(a).<sup>24</sup> Then, as the Mg chemical potential is increased, there

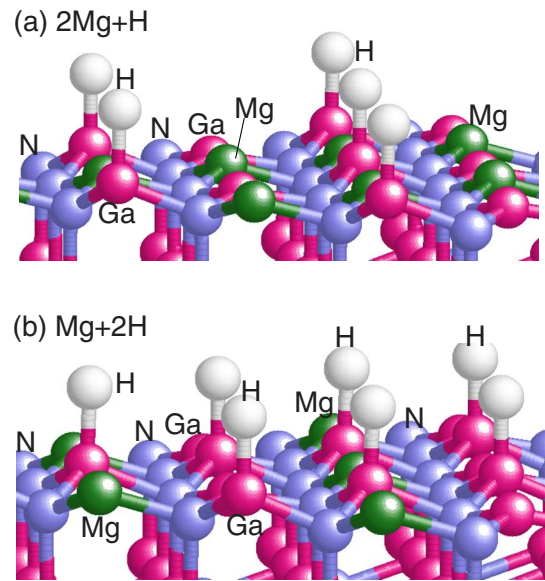


FIG. 4. (Color online) (a) Schematic model of the  $2 \times 2$   $c$ -plane  $2\text{Mg}+\text{H}$  surface. The structure has 0.5 ML of Mg replacing Ga atoms at the surface. (b) Schematic model of the  $2 \times 2$   $c$ -plane  $\text{Mg}+2\text{H}$  surface. The structure has 0.25 ML of Mg replacing Ga atoms at the surface. Both surfaces satisfy electron counting with all Ga and Mg dangling bonds empty.

is a transition to the  $\text{Mg}+2\text{H}$  surface. The  $\text{Mg}+2\text{H}$  surface, shown in Fig. 4(a), has 0.25 ML of Mg substituting for Ga in the top layer and 0.5 ML of hydrogen bonded to Ga atoms. The N adatoms are lost in the transition. The electron counting rule is still satisfied, with the Mg and Ga dangling bonds completely empty. The transition occurs at  $\mu_{\text{Mg}} = -1.53$  eV, about 0.5 eV below the onset of  $\text{Mg}_3\text{N}_2$  precipitation. If  $\mu_{\text{Mg}}$  is increased further, then we see a transition to the  $2\text{Mg}+\text{H}$  surface at  $\mu_{\text{Mg}} = -1.36$  eV. The  $\text{Mg}+2\text{H}$  surface is shown in Fig. 4(b). Finally, as one approaches the Mg-rich limit, there is a transition to the 3Mg surface. The important point is that the presence of hydrogen enables Mg to occupy surface sites in growth conditions corresponding to a lower Mg chemical potential. Without H, the transition to a surface with Mg occurs at  $\mu_{\text{Mg}} = -1.33$  eV. With H present, the onset occurs at  $\mu_{\text{Mg}} = -1.53$  eV. This result, together with the fact that a fraction of Mg atoms present on the surface get trapped in the bulk as growth proceeds, explains the experimental observation<sup>3</sup> that doping can be obtained at a lower Mg flux when H is present. This model may also account for why H does not significantly alter the Mg doping level at high Mg flux.<sup>3</sup> In fact, we see that the surface Mg concentration is not strongly affected by hydrogen when  $\mu_{\text{Mg}}$  is higher than the transition level. It is reduced from 0.75 ML in the 3Mg structure to 0.5 ML for the  $2\text{Mg}+\text{H}$  model. Thus, if the fraction of Mg incorporated is similar in the two cases, the total doping level will be affected only slightly.

#### IV. Mg-RICH GaN(10 $\bar{1}$ 0) SURFACES

Let us now consider Mg doping in growth on the GaN(10 $\bar{1}$ 0) surface, the  $m$  plane. We will show that H can

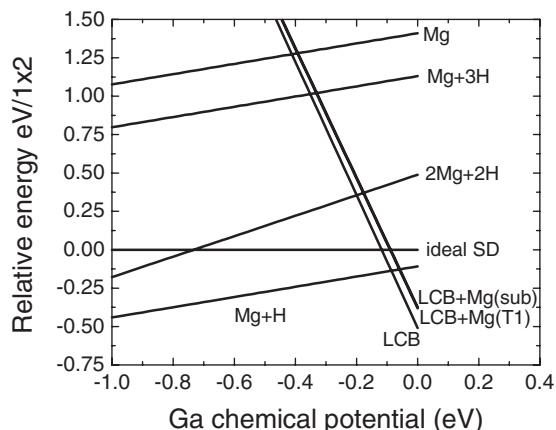


FIG. 5. Relative energies for GaN(1010) surfaces are plotted as a function of the Ga chemical potential. Results correspond to the Mg-rich limit, with  $p_{\text{H}}=10^{-10}$  atm and a temperature of 900 K, conditions for which  $\mu_{\text{H}}=-1.54$  eV. In these conditions, the Mg+H surface is stable from the N-rich limit until  $\mu_{\text{Ga}}>-0.1$  eV, at which point the laterally contracted bilayer model becomes the most stable. The ideal stoichiometric dimer surface is taken as the reference. The structure labeled Mg corresponds to 0.5 ML of Mg replacing Ga but with no H and is seen to be very high in energy. The Mg+3H and 2Mg+2H surfaces are not favorable in these conditions because the hydrogen chemical potential is too low. The chemical potential of Ga varies in the range  $\mu_{\text{Ga(bulk)}}+\Delta H<\mu_{\text{Ga}}<\mu_{\text{Ga(bulk)}}=0$ . The calculated heat of formation is  $\Delta H(\text{GaN})=-0.9$  eV.

play a significant role in this case as well. A key experiment here is that of McLaurin *et al.*, who investigated growth on the  $m$  plane and found that bulk Mg incorporation was enhanced by a factor of  $\sim 5$  under N-rich conditions in comparison to Ga-rich conditions.<sup>25</sup> To understand these observations, we consider the energetics of GaN(1010) surfaces in the presence of Mg and H. To simulate this MBE growth environment, the partial pressure of hydrogen will (as before) be set at a very low value,  $p_{\text{H}}=10^{-10}$  atm. The temperature will be set to  $T=900$  K, the temperature employed by McLaurin *et al.*<sup>25</sup> At this temperature and pressure, the chemical potential of hydrogen is very low,  $\mu_{\text{H}}=-1.54$  eV. The relative formation energies of various  $m$ -plane surfaces are shown in Fig. 5 as a function of the Ga chemical potential. The energies shown there correspond to the Mg-rich limit. In the absence of any Mg, the hydrogen chemical potential is sufficiently low that hydrogen is not stable on the surface. However, when Mg is introduced, a new structure forms that is very stable and involves Mg and H. This structure, the Mg+H structure, is shown in Fig. 6. In the Mg+H structure, one of the Ga atoms in the surface Ga-N dimer is replaced by a Mg atom, and the N atom in the dimer binds to a hydrogen atom. Note that the same structure but without the H atom is quite high in energy. The high energy of that structure is indicated by the line labeled Mg in Fig. 5. The Mg+H motif can be employed to create  $1\times n$  reconstructions by replacing  $1/n$  ML of Ga by Mg. Total energy calculations for Mg+H structures with  $\theta_{\text{Mg}}=1$  and  $\theta_{\text{Mg}}=0.5$  have been calculated by employing the  $1\times 2$  unit cell. The energies obtained for these two structures, denoted 2Mg

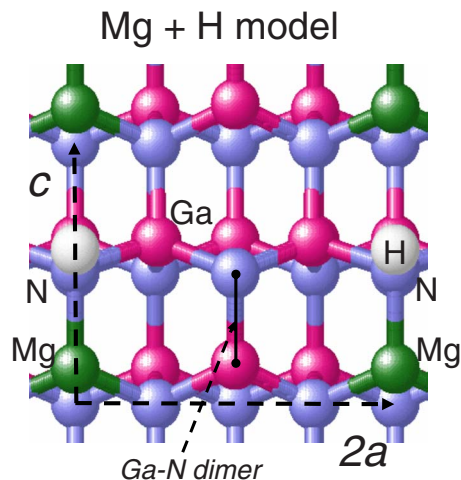


FIG. 6. (Color online) The Mg+H model for the GaN(1010) surface is shown. A surface Ga atom is replaced by Mg, and the neighboring N atom is capped by H atom to satisfy the electron counting rule. The lattice vectors  $\mathbf{c}$  and  $2\mathbf{a}$  are shown. In the 2Mg+2H model, both Ga atoms are replaced by Mg, and there are two H atoms per cell capping off the N atoms. In the Mg+3H surface, the Ga-N dimer is saturated by H atoms. For the Mg structure, one Mg substitutes for a Ga, as for the Mg+H structure, but no H is present. In the 4H surface, all surface atoms, four in each  $1\times 2$  cell, are capped by H.

+2H and Mg+H, are included in Fig. 5. The Mg+H structure is much more stable than any other surface in N-rich conditions. It is quite likely that the Mg+H structure is responsible for the Mg doping that is observed on the  $m$  plane in N-rich conditions. We suggest that in the MBE growth of  $m$ -plane GaN, the surface concentration of Mg is of order of 0.5 ML, and that a fraction of these Mg atoms become incorporated in bulk sites as the growth proceeds.

Let us now consider Mg incorporation on the  $m$  plane in Ga-rich growth conditions. On the basis of previous studies, the GaN(1010) surface is believed to adopt a Ga-adlayer type of reconstruction under Ga-rich conditions.<sup>26,27</sup> This surface is thought to contain more than 2 ML of Ga in a wetting layer. In the extreme Ga-rich limit, this wetting layer would be in equilibrium with Ga droplets. A low energy model for this type of surface is shown in Fig. 7. Although this model is not intended to be correct in every detail, it is expected to have most of the features of the minimum energy model for Ga-rich conditions. In the model, there are two adlayers of Ga above the stoichiometric dimer surface. One of the Ga adlayers (denoted the T layer) is bonded directly atop the N atoms in the surface dimers. The upper Ga adlayer (the A layer) is contracted along the  $[11\bar{2}0]$  direction so that the linear density in this row is increased by  $f=16.7\%$ . The contraction reduces the spacing between Ga atoms in this row to about 2.72 Å. The row-to-row registry of the A layers is then adjusted. Adjacent rows are shifted along the  $[11\bar{2}0]$  direction by  $3\mathbf{a}$ , so that the periodicity in the  $[0001]$  direction is  $2\mathbf{c}$ . This shift is expected to minimize frustration effects in the lateral relaxation of the atoms in the T layer. This gives rise to a  $c(2\times 6)$  reconstruction having 2.17 ML of Ga above the stoichiometric dimer. By adjusting the contraction factor

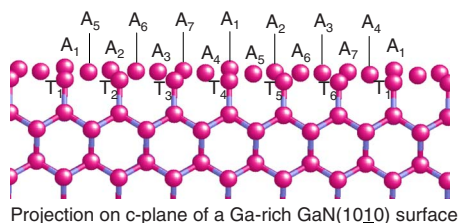


FIG. 7. (Color online) Shown is a model for the *m* plane in Ga-rich conditions. The model is similar to those discussed previously (Refs. 26 and 27). The present model has a compression in the A layer. All atoms visible in this projection are Ga. The Ga atoms in the (uncompressed) T layer are bonded strongly to N atoms in the layer below. The average spacing between Ga atoms in the A layer is contracted along the  $[11\bar{2}0]$  direction by  $f=16.7\%$ . Two rows of A-layer atoms are visible because of the row-to-row shift in registry. By adjusting the registry and  $f$ , more complex patterns may be formed, including one consistent with the observed unit cell (Ref. 26).

and the row-to-row registry, a structure consistent with the experimentally observed unit cell can be achieved.<sup>26</sup> As seen in Fig. 5, the formation energy of the  $c(2 \times 6)$  structure (denoted LCB) is less than the stoichiometric dimer surface (denoted ideal SD) by a substantial amount in Ga-rich conditions. It is important to note that the  $c(2 \times 6)$  LCB structure becomes more stable than the Mg+H surface in Ga-rich conditions. It is therefore expected that the formation of a Ga-adlayer surface will, to some extent, inhibit Mg incorporation in Ga-rich conditions. This is consistent with a reduction in the Mg doping level seen experimentally in Ga-rich conditions.<sup>25</sup> Calculations for  $c(2 \times 6)$  bilayer structures in which some of the Ga atoms in the near-surface region are replaced by Mg indicate that such substitution is not costly in energy. In the region where the  $c(2 \times 6)$  bilayer structure is stable, the replacement of a Ga atom in the T1 adlayer by a Mg atom costs about 0.35 eV/atom. [The energy of this structure is indicated as LCB+Mg(T1) in Fig. 5.] Thus, it is likely that at least 1% of a monolayer of Mg is incorporated in the bilayer, and some of these Mg will eventually be incorporated into the bulk, so that Mg doping is reduced but not entirely eliminated in Ga-rich conditions.

## V. METAL-ORGANIC CHEMICAL VAPOR DEPOSITION CONDITIONS: *m*-PLANE AND *c*-PLANE GROWTH

Let us now discuss the case of Mg incorporation in MOCVD growth conditions. It is important to note that Mg-doped *p*-type GaN layers are typically grown at a temperature of around 900 °C, a somewhat lower temperature than employed to grow undoped material. In the case of MOCVD growth, the nitrogen is supplied by thermally induced decomposition of a high pressure gas of  $\text{NH}_3$ . We consider high pressure growth conditions, in which the total reactor pressure is 1 atm, the partial pressure of  $\text{NH}_3$  is equal to 0.9 atm, and the partial pressure of  $\text{H}_2$  is equal to 0.1 atm. Employing temperature and pressure dependent calculations<sup>19</sup> for the chemical potential of  $\text{NH}_3$  and  $\text{H}_2$ , one can estimate the N

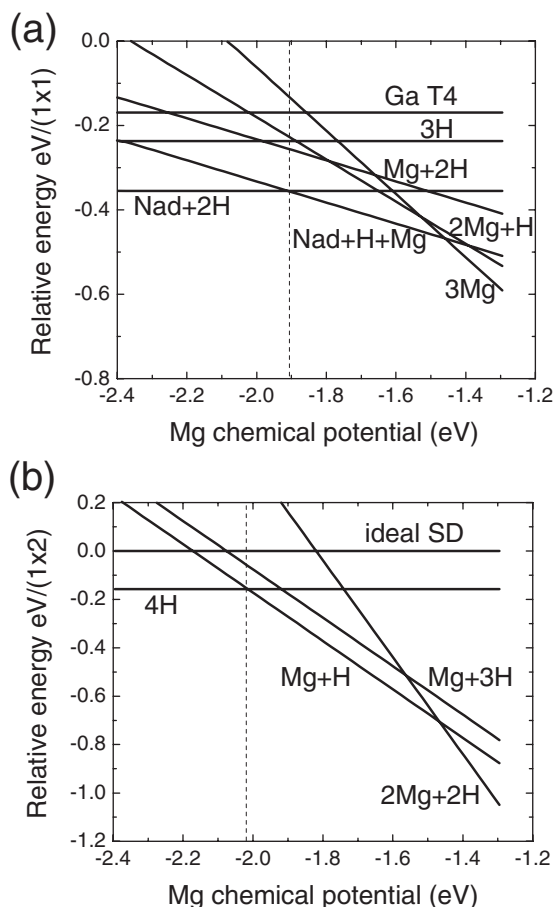


FIG. 8. Formation energies of (a) *c*-plane and (b) *m*-plane surfaces for MOCVD growth conditions employed to obtain *p*-type doping with Mg. ( $T=1170$  K,  $p_{\text{H}_2}=0.1$  atm, and  $p_{\text{NH}_3}=0.9$  atm.) This corresponds to  $\mu_{\text{Ga}} - \mu_{\text{Ga}(\text{bulk})} = -0.6$  eV and  $\mu_{\text{H}} = -1.0$  eV. The formation energies are given as a function of the Mg chemical potential. For the *c* plane the onset of Mg incorporation occurs with the stabilization of the  $\text{N}_{\text{ad}} + \text{H} + \text{Mg}$  surface. For the *m* plane, the onset occurs when the Mg+H surface becomes stable with respect to the hydrogen saturated surface (4H).

and Ga chemical potentials by assuming equilibration between  $\text{NH}_3$ ,  $\text{H}_2$ , and bulk GaN. For these conditions,  $\mu_{\text{H}} = -1.0$  eV. Using the relation  $\mu_{\text{N}} + \mu_{\text{Ga}} = \mu_{\text{GaN}(\text{bulk})}$ , we obtain  $\mu_{\text{Ga}} - \mu_{\text{Ga}(\text{bulk})} = -0.6$  eV. We therefore have a relatively N-rich growth environment, as is presumed in most studies.

Results for the *c* plane are shown in Fig. 8(a). The temperature is taken to be 1170 K in these calculations, corresponding to the temperature employed in the growth of the *p*-type layers. For low Mg chemical potential, the clean GaN surface that is the most stable in these conditions is the  $\text{N}_{\text{ad}} + 2\text{H}$  surface shown in Fig. 1(a). As the chemical potential of Mg increases, there is a transition (at  $\mu_{\text{Mg}} = -1.9$  eV) to the  $\text{N}_{\text{ad}} + \text{Mg} + \text{H}$  surface shown in Fig. 1(b). In the  $\text{N}_{\text{ad}} + \text{Mg} + \text{H}$  structure, one of the Ga atoms that was bonded to the nitrogen adatom has been replaced by Mg.<sup>28</sup> In addition, the H that was capping the Ga rest atom is removed so that the structure satisfies electron counting requirements. At still higher Mg chemical potentials, there is a transition to the 3Mg surface. It should be noted that the 3Mg surface con-

tains no hydrogen. This eliminates one source of H that may be useful in facilitating capture of Mg in the bulk.

The energies of the relevant  $m$ -plane surfaces in conditions appropriate for Mg doping ( $T=1170$  K,  $p_H=0.1$  atm, and  $\mu_{\text{Ga}}-\mu_{\text{Ga(bulk)}}=-0.6$  eV) are shown in Fig. 8(b). For these conditions, the hydrogen saturated surface (4H) is most stable for low  $\mu_{\text{Mg}}$ . On the H-saturated  $m$  plane, all surface Ga and N atoms are bonded to H. This surface is denoted 4H because there are four hydrogen atoms in each  $1 \times 2$  unit cell, two bonded to N atoms and two bonded to Ga atoms. As the Mg chemical potential increases, the transition to the Mg+H surface occurs at  $\mu_{\text{Mg}}=-2.0$  eV. In this transition, the concentration of H on the surface is decreased from 1.0 to 0.25 ML. The Mg+H surface is stable until the transition to a surface with all surface Ga atoms replaced by Mg and all surface N atoms capped by hydrogen. This surface is denoted 2Mg+2H in Fig. 8(b). The transition from Mg+H to 2Mg+2H may involve stable intermediates. It is possible that simple mixtures of the two structures, with  $0.5 < \theta_{\text{Mg}} < 1.0$ , may exist near  $\mu_{\text{Mg}}=-2.0$  eV, where the transition occurs in Fig. 8(b). In any event, there is a significant amount of H present on the surface in the Mg-rich limit.

These results show that Mg incorporation can be achieved on both the  $m$  plane and  $c$  plane in MOCVD growth conditions. However, there may be some advantages to doping on the  $m$  plane in comparison to the  $c$  plane. We note that the Mg chemical potential that is required to stabilize a surface containing Mg is lower on the  $m$  plane in comparison to the  $c$  plane. In addition, we note that in the Mg-rich limit, the surface concentrations of Mg on the  $m$  plane and  $c$  plane differ substantially. The 3Mg surface on the  $c$  plane gives rise to an areal Mg density of  $0.086$  Mg/ $\text{\AA}^2$ , whereas the  $m$ -plane 2Mg+2H surface has a Mg density of  $0.061$  Mg/ $\text{\AA}^2$ . Because Mg is a larger atom than the Ga it replaces, the higher Mg density present on the  $c$  plane creates a larger compressive stress. It is possible that this compressive stress is a driver of the growth instabilities and roughening that occur for heavily Mg-doped  $c$ -plane surfaces. These results suggest that heavy  $p$ -type doping on the  $m$  plane can be achieved with a lower probability of forming Mg-rich extended defects.

## VI. SUMMARY

The thermodynamics of hydrogen and magnesium incorporation on GaN  $c$ -plane and  $m$ -plane surfaces was investi-

gated via first-principles total energy calculations. On the basis of the results, an explanation was provided for why the presence of hydrogen allows Mg to be incorporated on the  $c$  plane at a reduced Mg flux.<sup>3</sup> When hydrogen is present, one may attribute the onset of Mg incorporation to a transition from the  $N_{\text{ad}}+2\text{H}$  surface to the Mg+2H surface that occurs at a Mg chemical potential of  $\mu_{\text{Mg}}=-1.53$  eV. In the absence of hydrogen, a transition to a surface that has a significant concentration of Mg occurs only for a higher chemical potential,  $\mu_{\text{Mg}}=-1.33$  eV. Consequently, Mg doping occurs for a lower Mg flux when hydrogen is present. The explanation supposes the validity of a model in which the doping occurs by kinetic capture of dopants into the bulk from the dopant-rich surface layer. Such a model is expected to be applicable at the temperatures employed typically in MBE growth of GaN.<sup>21</sup>

Our calculations show that hydrogen has a large effect on the stability of Mg-rich reconstructions of the  $m$  plane. On this basis we propose that the Mg doping of  $m$ -plane GaN grown in N-rich conditions by MBE (Ref. 25) involves the formation of the Mg+H surface. This surface is stable even when the hydrogen partial pressure is as low as  $10^{-10}$  atm. Under more Ga-rich conditions, the formation of the Mg+H surface is inhibited by the formation of a Ga-adlayer reconstruction. A Ga-adlayer structure with  $2.17$  ML of excess Ga and having  $c(2 \times 6)$  symmetry was shown to be stable in Ga-rich growth conditions. Since Mg incorporation is inhibited by the formation of the Ga-adlayer surface, Mg doping would be expected to be less in Ga-rich conditions in comparison to N-rich conditions. This picture seems to be consistent with experiments.<sup>25</sup>

In conditions appropriate for the MOCVD growth of Mg-doped GaN, the  $c$  plane is predicted to exhibit the  $N_{\text{ad}}+\text{Mg}+\text{H}$  structure or the 3Mg structure, depending on the Mg chemical potential. Under the same conditions, the  $m$  plane is predicted to adopt the Mg+H or 2Mg+2H structure. In the Mg-rich limit, the  $c$ -plane exhibits a structure with a higher areal density of Mg than does the  $m$  plane. The high areal density of Mg could be a driver of the instabilities that occur for heavily doped GaN  $c$ -plane surfaces. Thus, for very Mg-rich conditions, the  $m$  plane is expected to exhibit better surface morphology than the  $c$  plane.

## ACKNOWLEDGMENTS

The author is grateful to D. Bour, C. Chua, and N. Johnson for helpful discussions.

<sup>1</sup>V. Ramachandran, R. M. Feenstra, W. L. Sarney, L. Salamanca-Riba, J. E. Northrup, L. T. Romano, and D. W. Greve, Appl. Phys. Lett. **75**, 808 (1999).

<sup>2</sup>B. Beaumont, S. Haffouz, and P. Gibart, Appl. Phys. Lett. **72**, 921 (1998).

<sup>3</sup>A. J. Ptak, T. H. Myers, L. T. Romano, C. G. Van de Walle, and J. E. Northrup, Appl. Phys. Lett. **78**, 285 (2001).

<sup>4</sup>S. Nakamura, M. Senoh, S. Nagahama, N. Iwasa, T. Yamada, T.

Matsushita, H. Kiyoku, and Y. Sugimoto, Jpn. J. Appl. Phys., Part 2 **35**, L74 (1996).

<sup>5</sup>K. Okamoto, H. Ohta, S. F. Chichibu, J. Ichihara, and H. Takasu, Jpn. J. Appl. Phys., Part 2 **46**, L187 (2007).

<sup>6</sup>M. C. Schmidt, K. C. Kim, R. M. Farrell, D. F. Feezell, D. A. Cohen, M. Saito, K. Fujito, J. S. Speck, S. P. DenBaars, and S. Nakamura, Jpn. J. Appl. Phys., Part 2 **46**, L190 (2007).

<sup>7</sup>W. Götz, N. M. Johnson, J. Walker, D. P. Bour, and R. A. Street,

- Appl. Phys. Lett. **68**, 667 (1996).
- <sup>8</sup>S. Nakamura, N. Iwasa, M. Senoh, and T. Mukai, Jpn. J. Appl. Phys., Part 1 **31**, 1258 (1992).
- <sup>9</sup>J. Neugebauer and C. G. Van de Walle, Appl. Phys. Lett. **68**, 1829 (1996).
- <sup>10</sup>C. Skierbiszewski, Z. R. Wasilewski, M. Siekacz, A. Feduniewicz, P. Perlin, P. Wisniewski, J. Borysiuk, I. Grzegory, M. Leszczynski, T. Suski, and S. Porowski, Appl. Phys. Lett. **86**, 011114 (2005).
- <sup>11</sup>P. Vennéguès, M. Leroux, S. Dalmasso, M. Benaissa, P. De Mierry, P. Lorenzini, B. Damilano, B. Beaumont, J. Massies, and P. Gibart, Phys. Rev. B **68**, 235214 (2003).
- <sup>12</sup>W. Kohn and L. J. Sham, Phys. Rev. **140**, 1133 (1965).
- <sup>13</sup>R. Stumpf and M. Scheffler, Comput. Phys. Commun. **79**, 447 (1994).
- <sup>14</sup>D. M. Ceperley and B. J. Alder, Phys. Rev. Lett. **45**, 566 (1980).
- <sup>15</sup>N. Troullier and J. L. Martins, Phys. Rev. B **43**, 1993 (1991).
- <sup>16</sup>H. Monkhorst and J. Pack, Phys. Rev. B **13**, 5188 (1976). Calculations for  $1 \times 2 [c(2 \times 6)]$  unit cells on the  $m$  plane employ a  $4 \times 4 \times 1 [2 \times 2 \times 1]$  grid of  $\mathbf{k}$  points. For the  $2 \times 2$  calculations of the  $c$  plane, a  $4 \times 4 \times 1$  sampling grid is employed.
- <sup>17</sup>Guo-Xin Qian, R. M. Martin, and D. J. Chadi, Phys. Rev. B **38**, 7649 (1988).
- <sup>18</sup>J. E. Northrup, Phys. Rev. Lett. **62**, 2487 (1989).
- <sup>19</sup>J. E. Northrup, Appl. Phys. Lett. **86**, 122108 (2005).
- <sup>20</sup>J. E. Northrup, R. Di Felice, and J. Neugebauer, Phys. Rev. B **56**, R4325 (1997).
- <sup>21</sup>S. Guha, N. A. Bojarczuk, and F. Cardone, Appl. Phys. Lett. **71**, 1685 (1997). The observations that the concentration of incorporated Mg is independent of the arriving Mg flux and increases as the substrate temperature is reduced can be considered evidence for kinetic trapping of Mg atoms in a saturated surface phase.
- <sup>22</sup>J. E. Northrup, J. Neugebauer, R. M. Feenstra, and A. R. Smith, Phys. Rev. B **61**, 9932 (2000).
- <sup>23</sup>Q. Sun, A. Selloni, T. H. Myers, and W. A. Doolittle, Phys. Rev. B **73**, 155337 (2006). The 3Mg structure comprises 0.75 ML of Mg, with 0.5 ML in the top layer and 0.25 ML in third layer. Sun *et al.* found that this structure is more stable (by  $0.2 \text{ eV}/2 \times 2$ ) than the structure having 0.75 ML of Mg in the top layer. The present calculations confirm this result, giving an energy difference of  $0.17 \text{ eV}/2 \times 2$ .
- <sup>24</sup>C. G. Van de Walle and J. Neugebauer, Phys. Rev. Lett. **88**, 066103 (2002).
- <sup>25</sup>M. McLaurin, T. E. Mates, and J. S. Speck, Appl. Phys. Lett. **86**, 262104 (2005).
- <sup>26</sup>C. D. Lee, R. M. Feenstra, J. E. Northrup, L. Lympirakis, and J. Neugebauer, Appl. Phys. Lett. **82**, 1793 (2003). The experimental unit cell of the Ga-rich structure is  $\mathbf{e}_1 = 4\mathbf{a} + \mathbf{c}$ , and  $\mathbf{e}_2 = -\mathbf{a} + 5\mathbf{c}$ .
- <sup>27</sup>C. D. Lee, R. M. Feenstra, J. E. Northrup, L. Lympirakis, and J. Neugebauer, *GaN and Related Alloys—2002* [Mater. Res. Soc. Symp. Proc. **743**, 293 (2002)] (Materials Research Society, Pittsburgh, 2002).
- <sup>28</sup>In a different version of the  $N_{\text{ad}} + \text{Mg} + \text{H}$  model, the Mg would replace the Ga rest atom. However, that structure is found to be less stable than the one shown in Fig. 1(b) by  $0.21 \text{ eV}/2 \times 2$ .